Multiple Quasi-equilibria of the ITCZ and the Origin of Monsoon Onset.
Part II: Rotational ITCZ Attractors

Winston C. Chao and Baode Chen[1]

Laboratory for Atmospheres, NASA/Goddard Space Flight Center, Greenbelt, Maryland

[1]Universities Space Research Association, Lanham, Maryland

April 2000

Corresponding Author Address
Mail Code 913
NASA/Goddard Space Flight Center
Greenbelt, Maryland 20771

winston.chao@gsfc.nasa.gov

Abstract

Chao's numerical and theoretical work on multiple quasi-equilibria of the intertropical convergence zone (ITCZ) and the origin of monsoon onset is extended to solve two additional puzzles. One is the highly nonlinear dependence on latitude of the "force" acting on the ITCZ due to earth's rotation, which makes the multiple quasi-equilibria of the ITCZ and monsoon onset possible. The other is the dramatic difference in such dependence when different cumulus parameterization schemes are used in a model. Such a difference can lead to a switch between a single ITCZ at the equator and a double ITCZ, when a different cumulus parameterization scheme is used. Sometimes one of the double ITCZ can diminish and only the other remain, but still this can mean different latitudinal locations for the single ITCZ.

A single idea based on two off-equator attractors for the ITCZ, due to earth's rotation and symmetric with respect to the equator, and the dependence of the strength and size of these attractors on the cumulus parameterization scheme solves both puzzles. The origin of these rotational attractors, explained in Part I, is further discussed. The "force" acting on the ITCZ due to earth's rotation is the sum of the "forces" of the two attractors. Each attractor exerts on the ITCZ a "force" of simple shape in latitude; but the sum gives a shape highly varying in latitude. Also the strength and the domain of influence of each attractor vary, when change is made in the cumulus parameterization. This gives rise to the high sensitivity of the "force" shape to cumulus parameterization. Numerical results, of experiments using Goddard's GEOS general circulation model, supporting this idea are presented. It is also found that the model results are sensitive to changes outside of the cumulus parameterization. The significance of this study to El Nino forecast and to tropical forecast in general is discussed.

1. Introduction

Through various specially designed numerical experiments with an aqua-planet general circulation model and theoretical arguments, Chao (2000, hereafter C00) showed the existence of multiple quasi-equilibria of the intertropical convergence zone (ITCZ). He also showed that the onset of monsoon could be interpreted as an abrupt transition between the quasi-equilibria of the ITCZ. He further showed that the origin of these quasi-equilibria is related to two different types of attraction pulling the ITCZ in opposite directions. One attraction (or, "force" as explained in C00) on the ITCZ is due to earth's rotation, which pulls the ITCZ toward the equator or an equatorial latitude depending on the choice of convection scheme, and the other due to the peak of the sea surface temperature (SST, which is given in the experiments a Gaussian profile in latitude and is uniform in longitude), which pulls the ITCZ toward a latitude just poleward of the SST peak. The strength of the attraction due to the earth's rotation has a highly nonlinear dependence on the latitude and that due to the SST peak has a linear (at least in a relative sense; see C00 for discussion) dependence on the latitude. Fig. 1 (same as Fig. 8.a of C00) shows these two types of attraction when the Manabe convective adjustment scheme is used in the model. Curve R (positive means southward) is the attraction due to earth's rotation and line S (positive means northward) is the attraction due to SST peak when the SST peak is just south of the latitude where line S intersects the x-axis. Line S intersects curve R at three places. These are the quasi-equilibria; the outer two are stable and are the two possible locations for the ITCZ. When the SST peak is close to the equator, or when line S is replaced by line S2, there is only one quasi-equilibrium (point A in Fig. 1) which is on the equator side of the SST peak and which moves poleward at a slower rate when the SST profile is moved poleward while maintaining its

Gaussian shape. As the SST profile is moved poleward, line S moves poleward and (more or less) keeps its slope, quasi-equilibria B and C appear but the state remains at A. As the SST peak continues to gain latitude it will come to a point that point A disappears and the state (or the ITCZ), being pulled by the difference between curve R and line S, moves rapidly toward point C. Such rapid change of latitude of the ITCZ was interpreted in C00 as monsoon onset. The shape of curve R was confirmed by experiments; see Figs. 10 and 11 of C00 and their associated discussions. Fig. 2 (same as Fig. 8.c of C00) gives the diagram for curve R when the relaxed Arakawa and Schubert scheme (Moorthe and Suarez 1992, hereafter RAS) is used. Curve R takes on a very different shape; it is now the combination of the "forces" of the two attractors located at 13N&S[1]. It intersects the x-axis at three locations: the one at the equator is an unstable quasi-equilibrium and the other two are stable quasi-equilibria. The monsoon onset sequence in the case of RAS, which involves double ITCZ in the off-monsoon period, was described in C00. The shape of curve R was established through specially designed experiments; see Figs. 7, 11, and 13 of C00 and their associated discussions.

There are two important experimental facts discovered but unexplained in C00. One is the shape of curve R, or the highly nonlinear nature of the dependence of curve R on latitude. When the Manabe scheme is used, curve R, shown in Fig. 1, rises from zero at the equator with the latitude, reaches a maximum at about 8 or 9 degrees N, drops rapidly to near zero at about 14 N and then again rises sharply northward at a rate much higher than that at the equator. It is antisymmetric with respect to the equator. It is this highly nonlinear dependence that makes the multiple quasi-equilibria of the ITCZ and monsoon onset possible. The other unexplained fact is the drastic difference in the shape of curve R when different cumulus parameterization schemes

[1] C00 reported 17N&S based on experiments of shorter duration. Longer experiments showed locations closer to the equator.

are used (i.e., the different shape of curve R in Figs. 1 and 2). When RAS is used, curve R drops from zero at the equator with increasing latitude till it reaches a low at around 7 degrees N and then increases northward. This was also deduced from an experiment reported in C00 (see the discussion associated with Fig. 13 of C00.) Because of the different shape of curve R the model gives (as reported in C00), when SST is globally uniform (i. e., line S is zero), the intersects of curve R and line S (or the x-axis) give a single ITCZ at the equator in the case of the Manabe scheme and a double ITCZ in the case of RAS (Fig. 1 of C00.) This feature remains when the SST takes on a Gaussian shape and its peak is not too strong (i. e., the slope of line S is not too high) and is in the equatorial region. These are very different results.

The purpose of this paper is to solve these two puzzles and thus to make our theory of monsoon onset more complete. The approach is the same as in C00; i.e., theoretical arguments supported by numerical experiments. The model used, an updated version of the model used in C00, is described briefly in Section 2. The change of model version is not crucial to this study and is made only to keep up with the model development effort at Goddard. Our conceptual idea, which solves these two puzzles, is described in Section 3. Section 4 describes the numerical experiments which support our conceptual idea. This paper is concluded with some remarks and a brief summary in the last section.

2. Model used

The latest version of the Goddard Earth Observing System general circulation model version 2 (GEOS-2 GCM) is used. A 4° (longitude) x5° (latitude) grid size and 20 levels are used with 4 levels below 850 mb. This model uses the discrete dynamics of Suarez and Takacs

(1995). The relaxed Arakawa-Schubert scheme (RAS, Moorthi and Suarez, 1992) is a main feature of the model. This scheme gives almost identical time-mean results as the original Arakawa-Schubert scheme at much reduced computational cost. RAS is used in conjunction with a rain-reevaporation scheme (Sud and Molod, 1988). The large-scale moist and dry convection remain the same as documented in Kalnay et al. (1983). In some experiments in this work RAS is replaced by the moist convective adjustment scheme of Manabe (1965). The boundary layer and turbulence parameterization, a level 2.5 second-order closure model, is that of Helfand and Labraga (1988). Long wave radiation package is that of Chou and Suarez (1994). Short wave radiation package is that of Chou (1992) and Chou and Lee (1996). The prognostic cloud water parameterization of Del Genio et al. (1996) is used. Sea surface temperature, ground wetness, sea ice and snow are from observations (for details, see Takacs, et al. 1994.) We will use only the aqua-planet version of this model with specified zonally uniform SST as in C00; thus some features of the model, such as land surface process parameterization (Koster and Suarez 1996) and gravity wave drag parameterization (Zhou et al. 1996), are not used.

3. Interpretation

C00 has shown that with temporally and globally uniform SST and solar zenith angle the model shows a single ITCZ at the equator when the Manabe scheme is used and double ITCZ at 13S and N when RAS is used. As explained in C00 under such settings, if earth's rotation is excluded, everywhere on the globe is the same and there is no favorite location for precipitation and the time mean precipitation should be uniform or that of Benard cell-like convection. When rotation is included, precipitation does find favorite latitude due to two effects of rotation on

convection. As stated in C00, the first effect is the equivalence of rotation to vertical stratification with higher rotation corresponding to greater vertical stratification (Veronis 1967). A simple way to understand this equivalence is by first noting that convection is associated with convergence at low-levels and divergence at high-levels. When one takes the time derivative of the divergence equation and substitutes the time derivative of the vorticity term by that of the vorticity equation, one finds that the second time derivative of divergence δ is related to divergence itself with a coefficient of f squared and a negative sign, i.e.,

$$\frac{\partial^2 \delta}{\partial t^2} = -f^2\delta + \ldots$$

This equation, ignoring the other terms (which do not have the f factor) on the right hand side, has the same form as the equation that governs a spring. Like a spring that resists any pressing or stretching, rotation resists any convergence or divergence, which has the equivalent effect of resisting the vertical motion associated with convection (which is associated with low-level convergence and upper-level divergence), which in turn is the same as what stratification does to convection. This gives rotation an effect equivalent to stratification. Therefore the first effect of rotation favors the equator as the location for convection. Another way to understand this effect of rotation is to consider the frequency of inertial-gravity waves σ,

$$\sigma^2 = f^2 + N^2 \qquad (1)$$

where f is the Coriolis parameter and N^2 is the Brunt-Väisälä frequency squared which is $g\partial(\ln\theta)/\partial z$ in dry atmosphere, and θ is the potential temperature. In a saturated atmosphere N^2 is $g\partial(\ln\theta_e)/\partial z$, where θ_e is the equivalent potential temperature. The exact definition of N^2 for

unsaturated atmosphere is not a concern here. Suffice it to say that, without rotation, when N^2 turns negative, convection occurs. In the presence of rotation, when N^2 is everywhere the same and turns negative, the location where σ^2 turns negative first is the equator. Since f^2 can be added to N^2 (in Eq. 1), it must have the equivalent effect as the latter. Thus the ITCZ favors the equator because of rotation.

The second effect of rotation is, as stated in C00, that the boundary layer air converging toward the convective center picks up sensible and latent heat from the surface and this energy intake is increased by inflow's taking a longer inward-spiraling path with higher speed when rotation is present. Thus this second effect favors higher latitude for convection to occur. The compromise of the two effects favors locations at about 13 degrees S and N for the aqua-planet condition when RAS is used as determined by experiments in C00. These locations remain roughly the same when the Manabe scheme is used, as will be discussed. These locations can vary when the design of cumulus parameterization, boundary layer parameterization, or other aspects of the model is changed.

We can consider the locations of 13 degrees S and N as the centers of two attractors pulling on the ITCZ due to earth's rotation (which we name the rotational ITCZ attractors). The attraction (or the "force" as explained in C00) due to each attractor on the ITCZ is shown in Fig. 3 with positive values being southward. The "force" (or attraction) is zero at the center of the attractor and has different signs on the two sides of the center. Since the earth is not symmetric with respect to 13 degrees S or N, the "force" is not expected to be anti-symmetric with respect to the center. The magnitude of the "force" reaches a peak at some distance away and then falls at greater distance. The rise of the "force" from zero at the center of the attractor is assumed to be of sinusoidal type and the fall at greater distance is assumed to be of exponential type. There

is experimental support for such assumption (see discussion associated with Fig. 13 of C00), in the sense that deductions based on these assumptions fit experimental results. Theoretically, these assumptions are reasonable because the "force", due to the finite size of the attractors, has to diminish at greater distance. Although we can say that the scale of the attractors (or, the latitudinal distance from the center of the attractor to where the "force" is the largest) has something to do with the vigor of convection, exactly what determines it still awaits more theoretical work.

The combination of the two types of attraction (two "forces") is curve R. Fig. 2 (from Fig. 8.c of C00) shows such combination when RAS is used. The fact that the "force" of each attractor reaches a peak magnitude before reaching the equator has been demonstrated in C00 (see the discussion associated with the last figure in C00), where an experiment shows that when the Gaussian SST peak remains at the equator and becomes sharper, the double ITCZ symmetric with respect to the equator switches to a single ITCZ over the equator. If the attractors become stronger and wider or if the centers of the attractors move closer to the equator (say, when a different cumulus parameterization scheme is used, when some parameters in the scheme are tuned, or when some features in the model outside of the cumulus parameterization scheme are changed), the "force" peak location can be moved to the other side of the equator. The situation can change to give curve R a shape shown in Fig. 1. Fig. 4 shows such a combination. In Fig. 4 the slope of curve R at the equator is the same as the slope of the "force" at the equator due to either attractor. The latter is smaller than the slope of the "force" at the center of either attractor. Due to the rapid decline of the "force' due to the 13S attractor south of 13N, at 13N the slope of curve R is almost the same as that of the 13N "force" at its center. This explains why the rise of curve R north of 13N is greater than its rise at the equator. The sum of the two "forces" after

reaching a peak around 7N drops quickly poleward to give curve R a shape like what is shown in Fig. 1. Numerical experiment results will be presented in the next section to support the idea presented in this section.

4. Supporting numerical experiments

According to the idea in the preceding section, it is possible to make changes in a cumulus parameterization scheme and obtain a change in the shape of curve R from that in Fig. 2 to that in Fig. 1 or vice versa and this will results in a change in the stable quasi-equilibria, or a change between double ITCZ (or a single ITCZ away from the equator) and a single ITCZ at the equator. We will make a change in RAS, which is an addition of a condition to be met before cumulus convection is allowed to occur. The condition is that the boundary layer relative humidity has to be greater than a critical value, r_c. This condition was used by Wang and Schlesinger (1999) in a GCM to improve the simulation of the Madden-Julian oscillation. We found it also useful for our present purpose. Raising r_c gives a more intense ITCZ (because cumulus convection becomes harder to occur, and when it does occur it is more intense) and the rotational attractors become stronger and their "force" peaks (in absolute value) can cross the equator (starting from curve RS or RN in Fig. 2). The shape of curve R can change from that of Fig. 2 to that of Fig. 1 and correspondingly the two off-equator stable ITCZ quasi-equilibria change to one at the equator.

Fig. 5 shows the zonal mean precipitation averaged over the last 100 days of three 455 day experiments using RAS with uniform SST of 29°C with r_c equal to 0%, 90% and 95%. The initial conditions are the same as those in C00 and the solar angle is the globally averaged value.

In the first two experiments the curve R have the shape of Fig. 2 and the third experiment curve R has the shape of Fig. 1. Fig. 6 shows the ITCZ location of an experiment with uniform SST of 29°C where RAS is used and r_c is increased from 90% to 95% linearly in 100 days after a period of 200 days with r_c=90%. The ITCZ that starts out being away from the equator switches to the equator in a short period of 30 days. Fig. 7 is an identical experiment except the r_c values of 90% and 95% are switched. The ITCZ that starts out at the equator switches away from the equator; the switch in this case is much faster. The equatorial ITCZ regime in Figures 6 and 7 shows occasional split into double ITCZ structure (e.g., day 112 through day 160 in Fig. 7). However this structure, in which the ITCZ's are only 6 or 7 degrees away from the equator, is distinctly different from the ITCZ in the other regime (of rc=90%) where the ITCZ is 13 degrees away from the equator and exists in only one hemisphere. In the equatorial ITCZ regime there are also weaker rain bands located at 19-23 degrees in both hemispheres which oscillate in time with an intraseasonal periodicity (which are reflected in the dash line in Figure 5) and is weaker when the ITCZ at the equator becomes stronger. Although the reason for such a flow regime remains to be investigated, this result reveals the complexity and richness of the interaction between convection and large-scale circulations and the need for further refinement of our theory. The framework of this refinement is that the rotational ITCZ attractors we proposed should be considered as quasi-equilibria (as stated in C00) instead of fixed point attractors. Thus there can be small oscillation in time of the location, strength and shape of the attractors and it is these small oscillations that gives rise to a variety of complex flow patterns.

The shape of curve R is revealed, as in Fig. 10 of C00, by specifying the SST as a Gaussian profile as given by Eq. (1) in C00 and moving the SST profile slowly poleward (the peak of the SST, after being fixed at the equator for 100 days, moves from the equator to 30N

linearly in 276 days) for both 90% and 95% cases. Fig. 8 and 9 show these results and reveal the shape of curve R in the two cases to be those of curve R in Figs. 1 and 2 (Figs. 8 and 9 being similar to Figs. 10 and 12 of C00). Thus besides the confirmation that RAS can be modified to give both shape of curve R, we have made the additional discovery that the switch between the two shapes is a critical phenomenon.

Curve R, when RAS is used, can also be changed by removing surface friction. When the surface friction is removed, the boundary layer inflow direction becomes closer to the isobaric contours and the inflow takes a longer path than in the case with surface friction. As a result the second effect of rotation discussed in Section 3 becomes larger and the locations of the rotational ITCZ attractors become farther away from the equator. An experiment using RAS with uniform SST and without surface friction shows such a result (Fig. 10.) Fig 10 also shows the results of increasing surface friction by a factor of three. The northern ITCZ moves closer to the equator as expected, but the southern ITCZ moves away. The reason is not clear. Because the locations of the rotational ITCZ attractors (Fig. 2) are pushed further away from the equator, when the surface friction is removed, when the Gaussian SST profile with a peak at the equator is introduced only a single ITCZ at the equator is obtained. The dash line in Fig. 11 shows such results, which is in contrast with the case with surface friction (solid line in Fig. 11), which shows a double ITCZ.

The experience with removing surface friction in the RAS case suggests the possibility that the single ITCZ over the equator in the experiments using MCA can be transformed into a double ITCZ or a single ITCZ away from the equator by removing surface friction. Thus an experiment of 400 days long using MCA with uniform SST of 29°C and without surface friction was conducted. The result (Fig. 12) still remains as a single ITCZ at the equator. However the

single ITCZ is much broader in latitudinal direction (and is occasionally split into two with peaks very close to the equator.) This indicates that the slope of Curve R at the equator has become smaller. And this smaller slope is consistent with the moving apart of the two attractors. In Fig. 4 it is obvious that the slope of R at the equator is the same of the slope of either RS or RN at the equator and if the two attractors are moved apart the slope of R at the equator becomes smaller, which gives a less sharp ITCZ over the equator. Other attempts to obtain double ITCZ using MCA, such as changing critical relative humidity for convection to start, changing the Coriolis parameter, and changing radiative cooling rates, were also not successful.

5. Remarks and summary

Although we have demonstrated that with RAS the shape of the rotational ITCZ attractor "force" can be changed by tuning r_c and surface friction, other sensitive parameters in RAS need to be explored. How these parameters change RAS is an interesting topic. Why the attractors are wider in the case of MCA than in case of the RAS is also a question that should be investigated in the future. This may be related to the more vigorous precipitation rate in association with the individual convective cells when MCA is used, an indication that condition for convective onset is more stringent with MCA. The eventual solution of this question involves the understanding of the interaction between cumulus heating due to a convection scheme and the large-scale circulation. This interaction involves the Coriolis force. This situation points to the need of an analytic study of the attractor "force". Unfortunately such a study requires an analytic formula for cumulus parameterization, among other things, which is

presently unavailable. The use of the so-called wave-CISK heating formula is not advisable (Chao and Deng 1997).

When a double ITCZ is allowed, sometimes both ITCZ's appear but at other times only one ITCZ (or one is more stronger than the other) occurs. What decides the choice between the two possibilities is an interesting question. Our empirical answer is that when the model parameters are not symmetric with respect to the equator, the ITCZ that is in a more stable state, (i.e., the angle formed by the intersection of curve R and line S which covers the x-axis is larger) has the edge. When the model parameters are symmetric with respect to the equator, if that angle is large both ITCZ exists, otherwise only one random ITCZ exists.

Whether a model gives a single or double ITCZ or whether a single ITCZ is located at or away from the equator has a decisive impact on the equatorial surface winds which are crucial in the forecast of El Nino with a coupled model. Our investigation has shown the critical importance of the cumulus parameterization in simulating ITCZ and monsoon onset; therefore the importance of the cumulus parameterization to El Nino forecast or to tropical forecast in general is made obvious through this study. The experiment we did with changing the boundary layer relative humidity required for convection with RAS is but one example of how to modify the cumulus parameterization scheme. A clear direction for future research is to explore other ways, perhaps more physically meaningful ones, to improve the performance of the cumulus parameterization scheme. We must also point out that changing cumulus parameterization is not the only way to induce change between single and double ITCZ or change in the location of a single ITCZ; changing other parts of a model can have the same effect. However it does appear that changes in cumulus parameterization scheme can be more effective in inducing changes in ITCZ. The impact of modifying boundary layer parameterization in the context of tropical

forecast is another worthy direction. The effect of cloud-radiation interaction on the ITCZ and monsoon onset, though appearing to be relatively minor, needs to be assessed.

In summary this investigation has solved two puzzles encountered in C00; i.e., the highly nonlinear dependence of the attraction on the ITCZ due to earth's rotation and the high sensitivity of such dependence to the cumulus parameterization scheme used in the model. A single idea based on two off-equator attractors for the ITCZ due to the earth's rotation (the rotational ITCZ attractors) and the dependence of the strength and shape of these attractors on the cumulus parameterization scheme solves both puzzles. It is found that although the attracting "force" of each attractor may exhibit very simple structure, the combination of the two gives a sum highly varying in latitude and is highly varying when the cumulus parameterization scheme is modified or replaced. With the resolution of these two puzzles our interpretation for the origin of monsoon onset becomes more complete. Through the circulation field associated with the ITCZ and the role of cumulus parameterization scheme in determining the location of the ITCZ, this study shows why a good cumulus parameterization scheme is crucial for successful El Nino forecast and for tropical forecast in general.

Acknowledgments: This work was supported by NASA Earth Science Division with funds managed by Kenneth Bergman.

References

Chao, W. C., 2000: Multiple quasi-equilibria of the ITCZ and the origin of monsoon onset. *J. Atmos. Sci.*, **57**, 641-652.

Chao, W. C. and L. Deng, 1997: Phase-lag between deep cumulus convection and low-level convergence in tropical synoptic-scale systems. *Mon. Wea. Rev.*, **125**, 549-559.

Chou, M. D., 1992: A solar-radiation model for use in climate studies. *J. Atmos. Sci,* **49**, 762-772.

Chou, M. D., K.-T Lee., 1996: Parameterizations for the absorption of solar radiation by water vapor and ozone. *J. Atmos. Sci.,* **53**, 1203-1208.

Chou, M. D. and M. J. Suarez, 1994: An efficient thermal infrared radiation parameterization for use in general circulation models. NASA Tech Memo. 104606, Vol. 3.

Del Genio, A. D., M.-S. Yao, W. Kovari, and K. K.-W. Lo, 1996: A prognostic cloud water parameterization for general circulation models. *J. Climate*, **9**, 270-304.

Helfand, H. M., and J. C. Labraga, 1988: Design of a non-singular level 2.5 second-order closure model for the prediction of atmospheric turbulence. *J. Atmos. Sci.*, **45**, 113-132. Reply to comments, **46**, 1633-1635.

Kalnay, E., R. Balgovind, W. Chao, D. Edelmann, J. Pfaendtner, L. Takacs, and K. Takano, 1983: Documentation of the GLAS fourth-order general circulation model. Vol. 1: Model description. NASA Tech Memo 86064 (available from the library of NASA/Goddard Space Flight Center, Greenbelt, MD 20771).

Koster, R., and M. Suarez, 1996: Energy and water balance calculations in the Mosaic LSM. NASA Tech Memo. 104606, Vol. 9, 60 pp. (available from the library of NASA/Goddard Space Flight Center, Greenbelt, MD 20771).

Manabe, S., J. Smagorinsky, and R. F. Strickler, 1965: Simulated climatology of a general circulation model with a hydrological cycle. *Mon. Wea. Rev.*, **93**, 769-798.

Moorthi, S., and M. J. Suarez, 1990: Relaxed Arakawa-Schubert: A parameterization of moist convection for general circulation models. *Mon. Wea. Rev.*, **120**, 978-1002.

Suarez, M. J. and L. L. Takacs, 1995: Documentation of the Aries-GEOS dynamical core: Version 2 NASA/Tech Memo 104606, Vol. 5. (available from the library of NASA/Goddard Space Flight Center, Greenbelt, MD 20771)

Sud, Y. C. and A. Molod, 1988: The roles of dry convection, cloud-radiation feedback processes and the influence of recent improvements in the parameterization of convection in the GLA GCM. *Mon. Wea. Rev.*, **116**, 2366-2387.

Takacs, L. L., A. Molod, T. Wang: 1994: Documentation of the Goddard Earth Observing System (GEOS) General Circulation Model- Version 1. NASA Tech Memo 104606, Vol. 1. (available from the library of NASA/Goddard Space Flight Center, Greenbelt, MD 20771).

Veronis, G., 1967: Analogous behavior of rotating and stratified fluids. *Tellus*, **19**, 620-633.

Wang, W., and M. E. Schlesinger, 1999: The dependence on convection parameterization of the tropical intraseasonal oscillation simulated by the UIUC 11-layer atmospheric GCM. *J. Climate*, **12**, 1423-1457.

Zhou, J., Y. C. Sud, and K.-M. Lau, 1996: Impact of orographically induced gravity-wave drag in the GLA GCM. *Q.J.R. Meterorol. Soc.*, **122**, 903-927.

Figure Captions

Fig.1. Schematic diagram showing the two "forces" acting on the ITCZ when the Manabe scheme is used in the model. Curve R represents the "force" due to earth's rotation (positive means southward). Line S represents the "force" due to the SST (positive means northward). The SST has a Gaussian shape in latitude and is uniform in longitude and is given in Eq. (1) of C00.

Fig. 2. Same as Fig. 1 but for RAS. RS and RN are the "forces" due to the attractors at 13 degrees N and S, respectively. Curve R is the sum of RS and RN.

Fig. 3. The schematic shape of the attracting "force" due to an ITCZ attractor. The "force" (positive means southward) is zero at the center of the attractor and increases sinusoidally away from the center and falls exponentially after reaching a peak.

Fig. 4. The combination, R, of two rotational ITCZ attractors, RN and RS, with large domain of influence.

Fig. 5. Zonal mean precipitation averaged over the last 100 days of three 455 day experiments with uniform SST of 29°C and with the condition of boundary layer relative humidity being greater than 0% (solid), 90% (long dash) and 95% (short dash) imposed on RAS.

Fig. 6. Position of the ITCZ of an experiment with uniform SST using RAS and r_c is increased from 90% to 95% linearly in 100 days after a period of 200 days with r_c =90%. r_c is the critical relative humidity value above which cumulus convection is allowed.

Fig. 7. Identical to Fig. 6 except the values of r_c =90% and 95% are switched.

Fig. 8. Zonal mean precipitation in an experiment where the SST takes on a Gaussian profile and the profile is moved northward such that the SST peak moves from the equator to 30N in 276 days. r_c is 90%.

Fig. 9. Same as Fig. 8 but r_c =95%.

Fig. 10. Time and zonal mean precipitation for experiments using RAS with no surface friction (long dash), with no change in surface friction (solid) and with a factor of three multiplied to the surface friction coefficient (short dash).

Fig. 11. Latitudinal distribution of time-zonal mean precipitation of RAS experiments with Gaussian SST latitudinal profile centered over the equator with (solid line) and without (dash line) surface friction.

Fig. 12. Latitudinal distribution of time-zonal mean precipitation of MCA experiments with (solid) and without (dash line) surface friction. The SST is globally uniform.

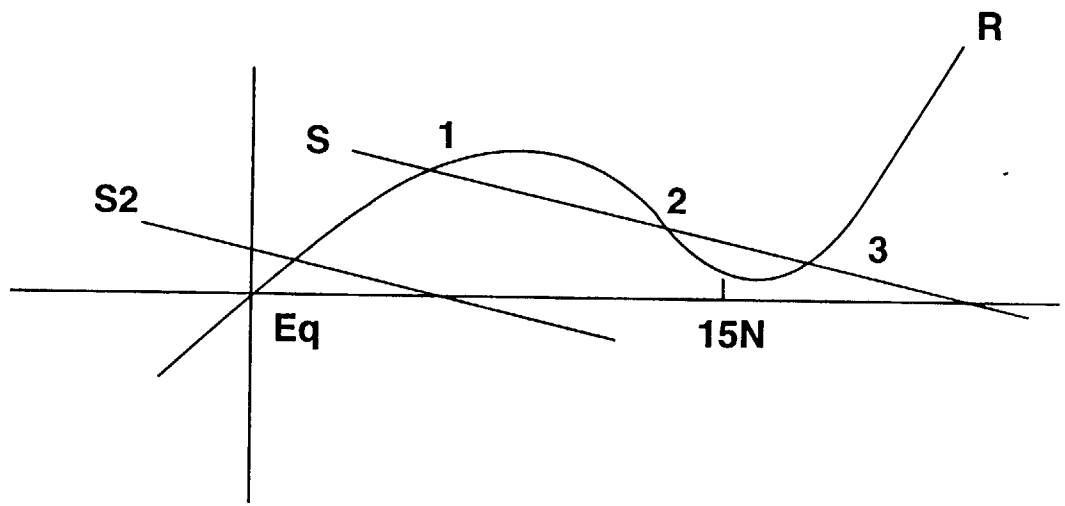

A1408.004

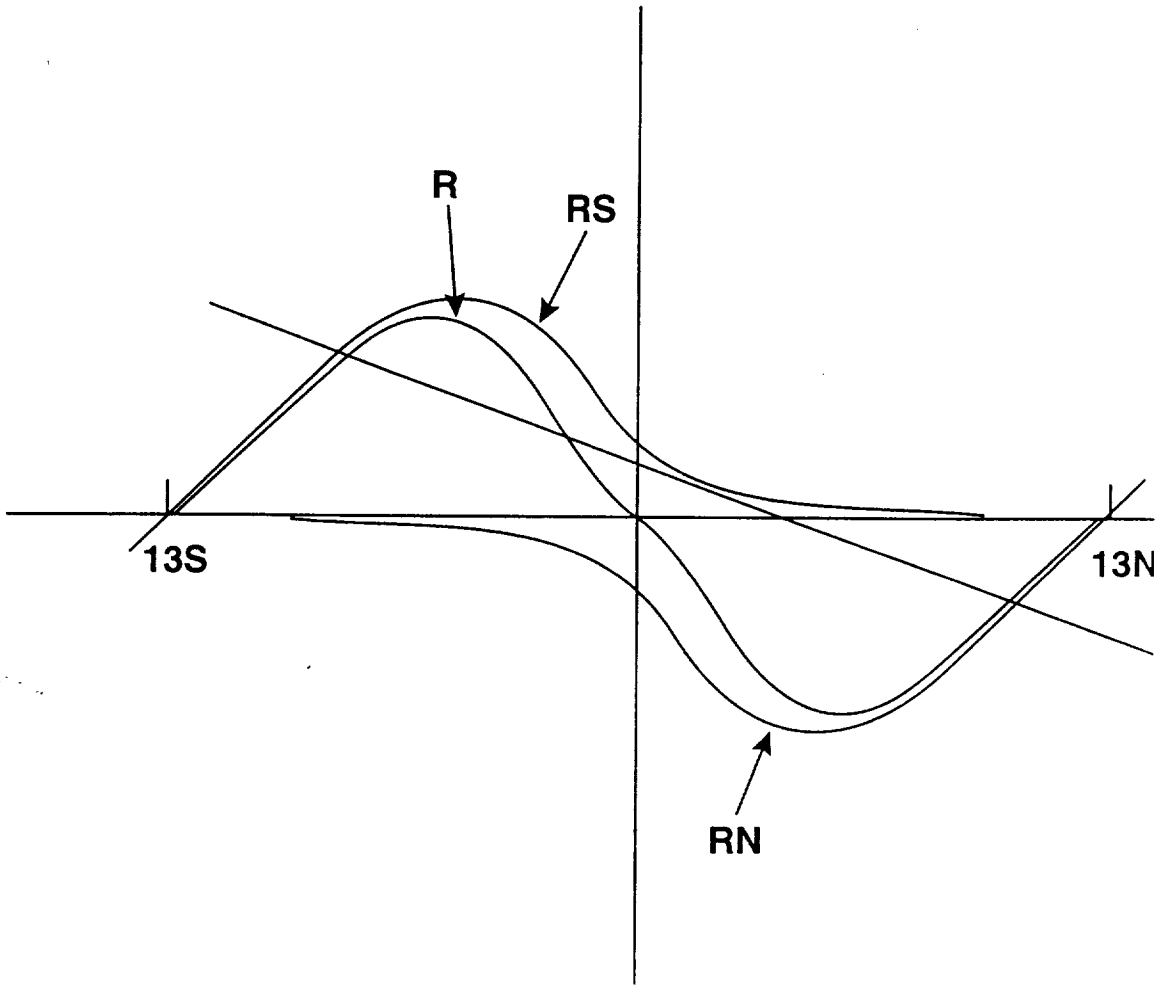
R
RS
13S
13N
RN

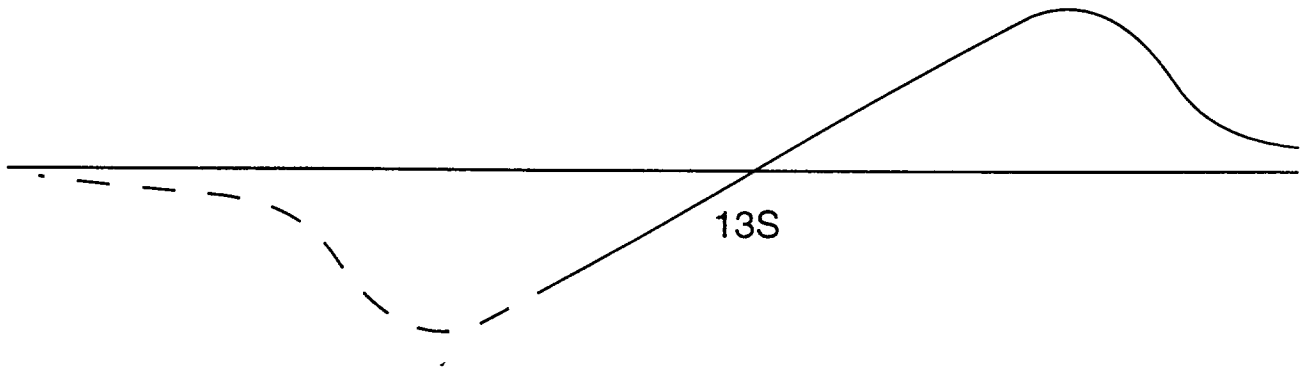
13S

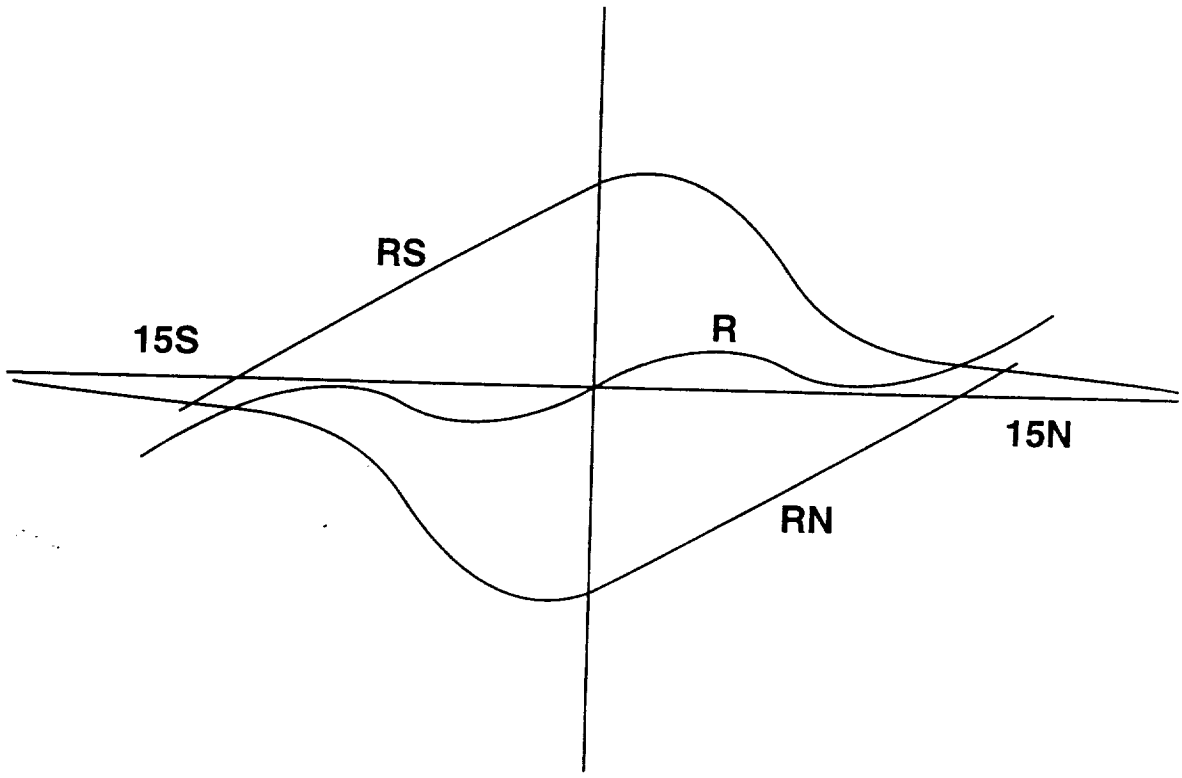
RS
15S
R
15N
RN

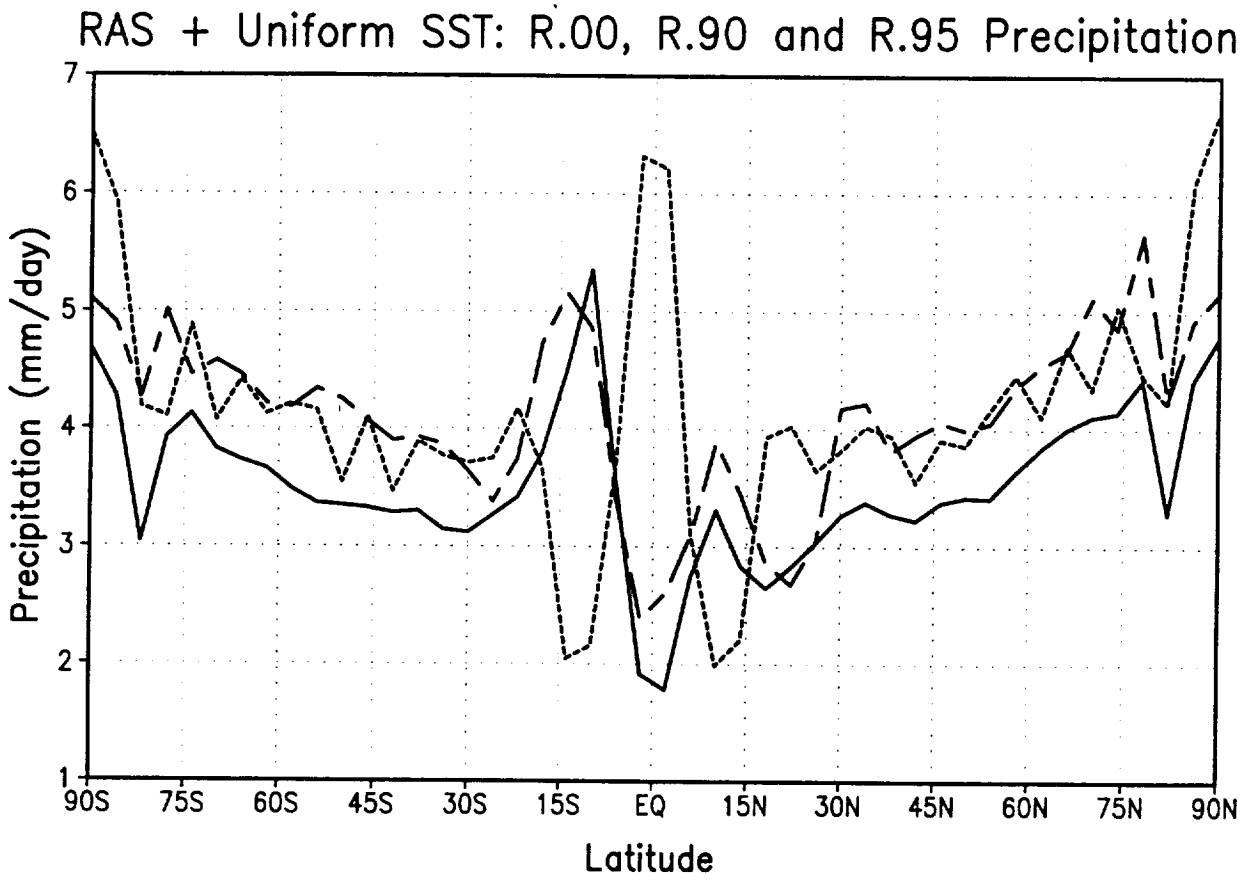
RAS + Uniform SST: R.00, R.90 and R.95 Precipitation
Precipitation (mm/day)
7
6
5
4
3
2
1
90S
75S
60S
45S
30S
15S
EQ
15N
30N
45N
60N
75N
90N
Latitude

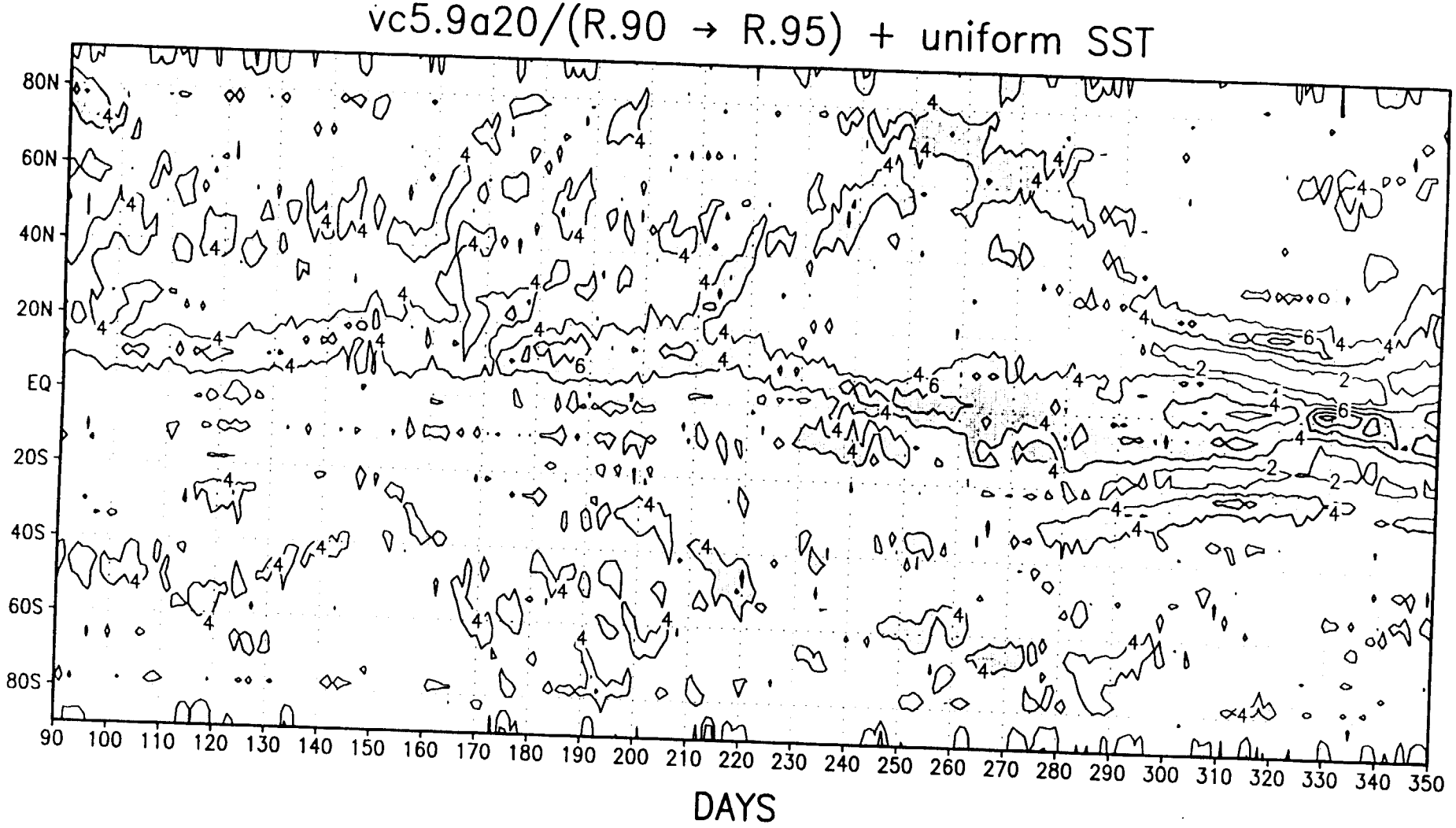
vc5.9a20/(R.90 → R.95) + uniform SST
80N
60N
40N
20N
EQ
20S
40S
60S
80S
90 100 110 120 130 140 150 160 170 180 190 200 210 220 230 240 250 260 270 280 290 300 310 320 330 340 350
DAYS

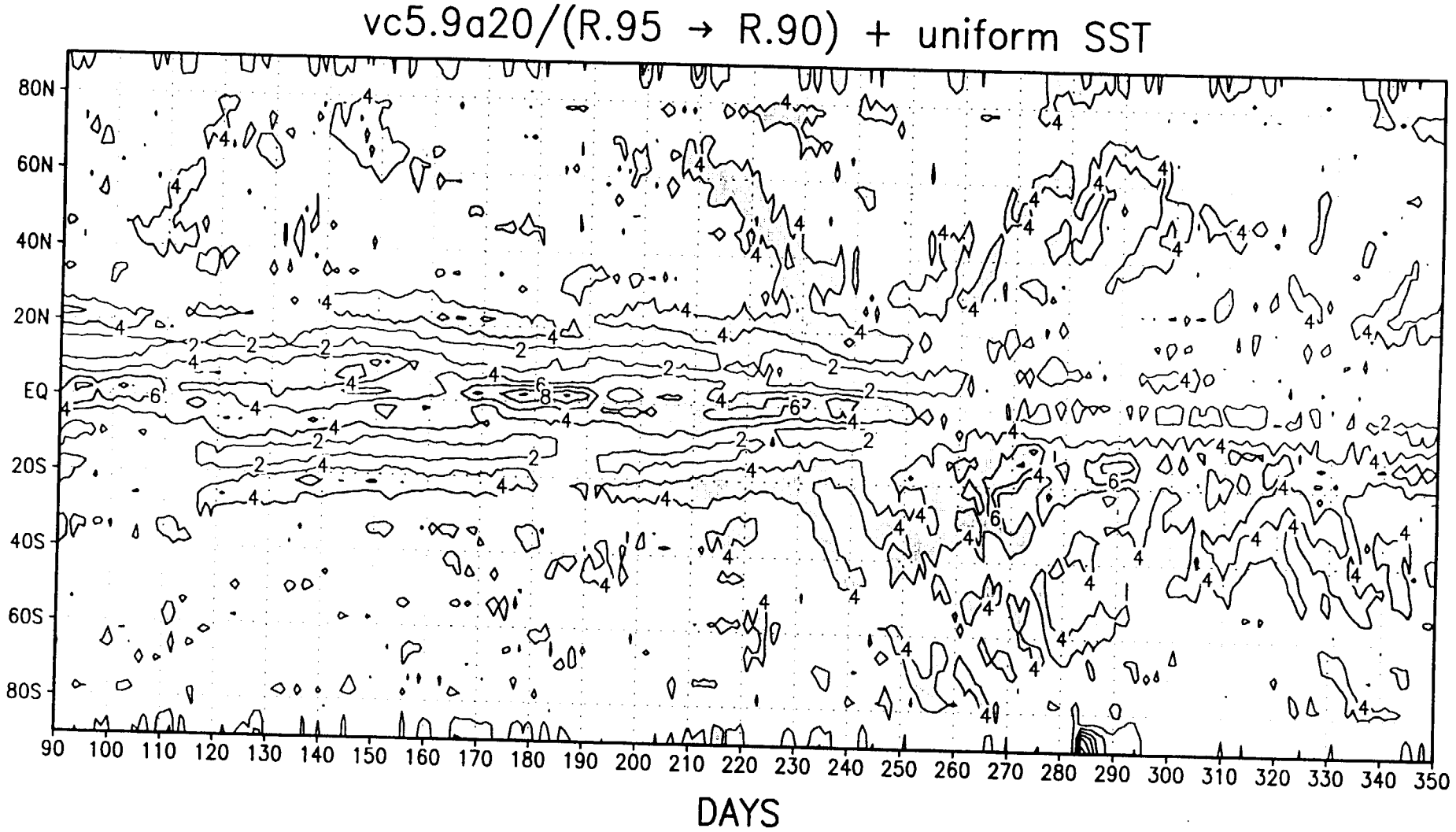
vc5.9a20/(R.95 → R.90) + uniform SST
80N
60N
40N
20N
EQ
20S
40S
60S
80S
90 100 110 120 130 140 150 160 170 180 190 200 210 220 230 240 250 260 270 280 290 300 310 320 330 340 350
DAYS

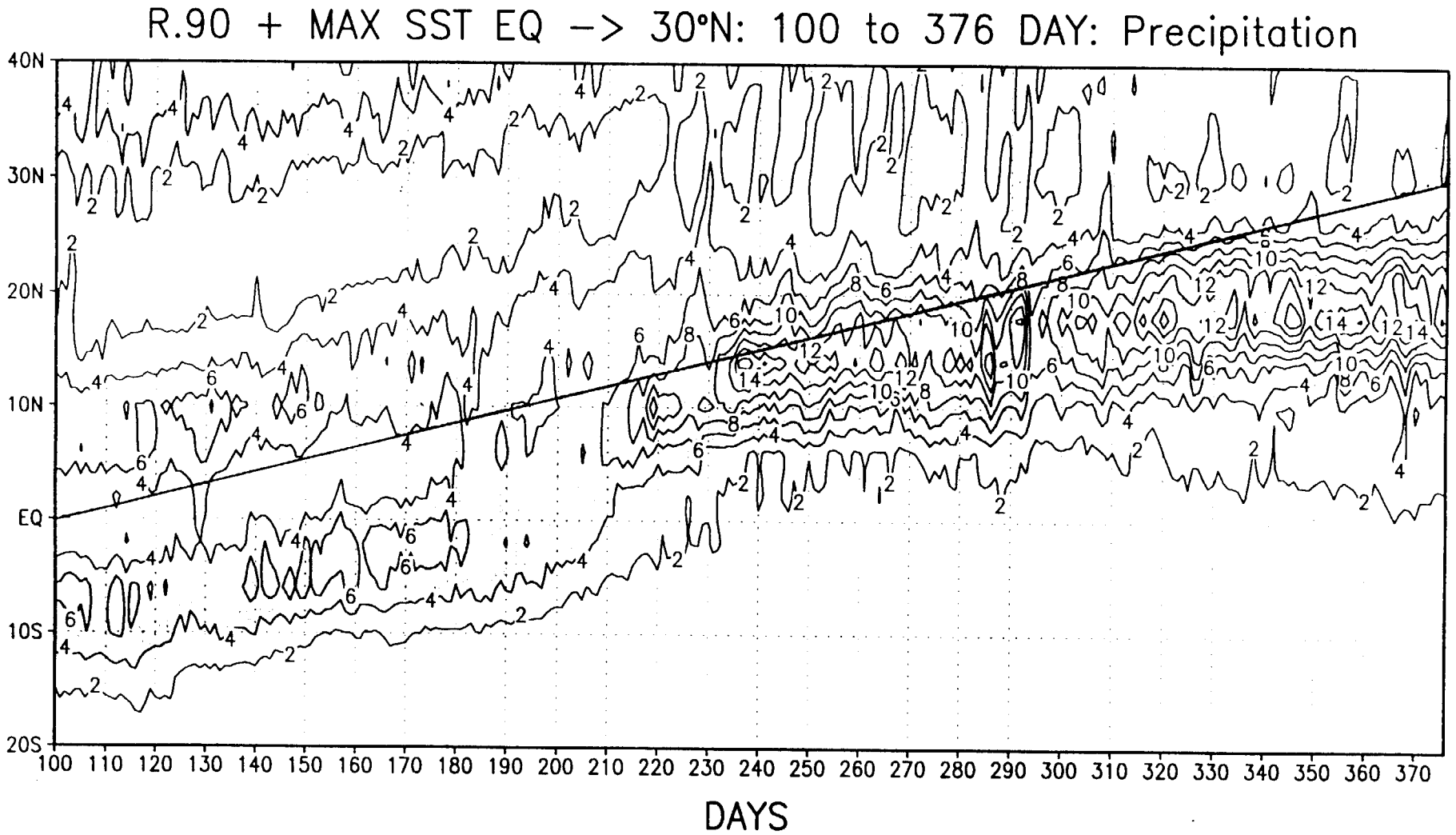
R.90 + MAX SST EQ -> 30°N: 100 to 376 DAY: Precipitation
40N
30N
20N
10N
EQ
10S
20S
100 110 120 130 140 150 160 170 180 190 200 210 220 230 240 250 260 270 280 290 300 310 320 330 340 350 360 370
DAYS

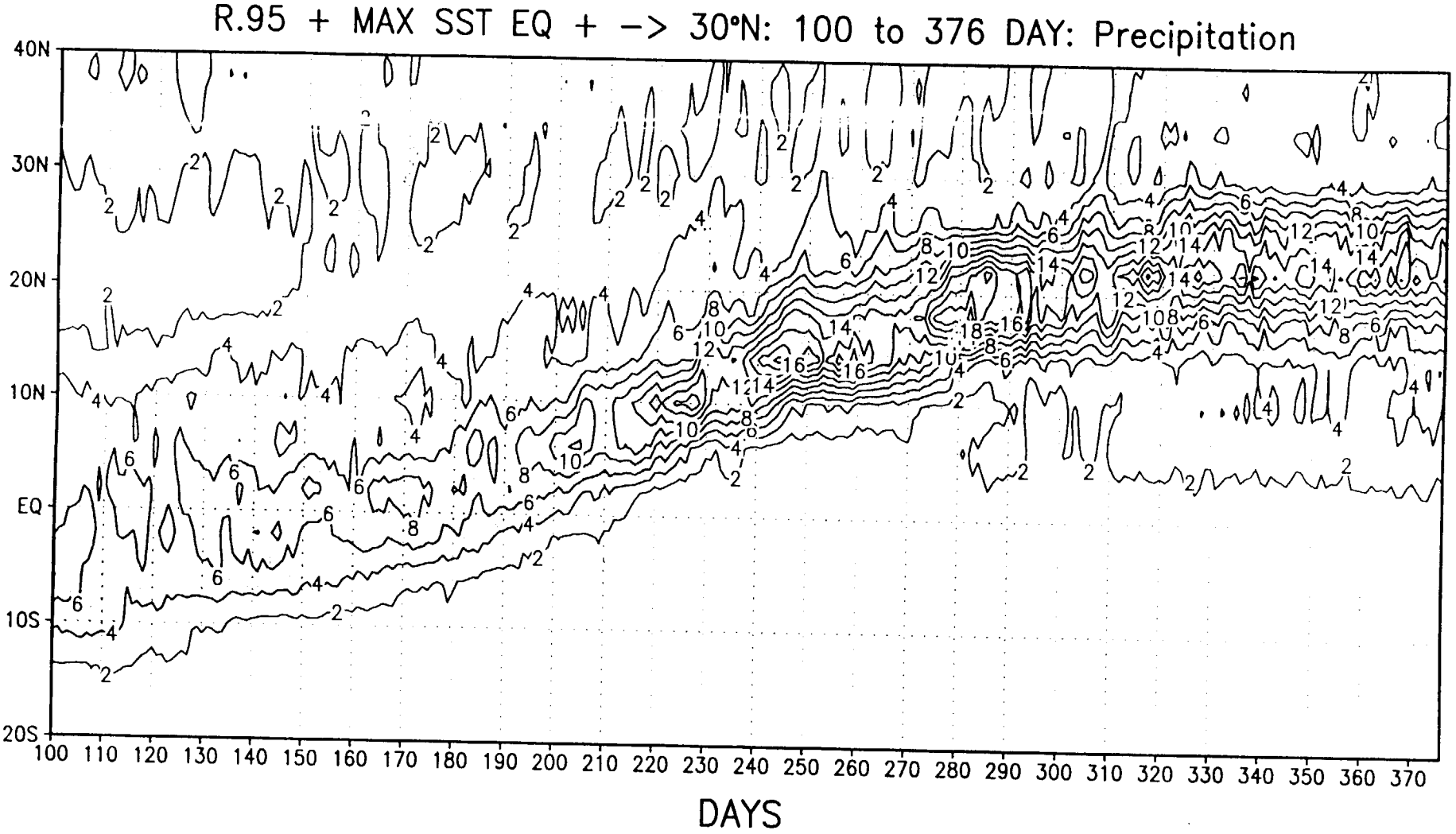
R.95 + MAX SST EQ + -> 30°N: 100 to 376 DAY: Precipitation
40N
30N
20N
10N
EQ
10S
20S
100 110 120 130 140 150 160 170 180 190 200 210 220 230 240 250 260 270 280 290 300 310 320 330 340 350 360 370
DAYS

w/ 3.0&1.0&0.0*sfc friction + R.00 + Uniform SST (355–455 days): Precip.

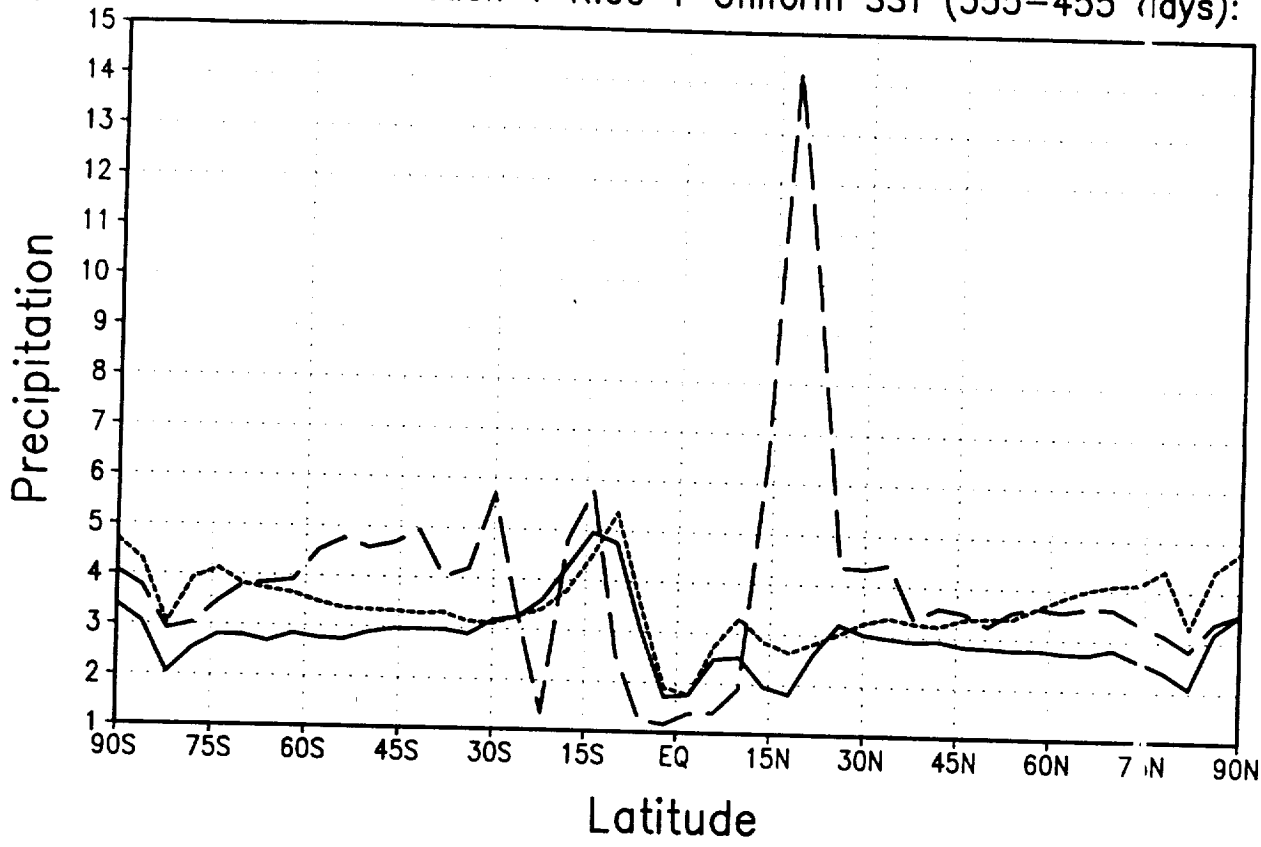

Long dash no sfc friction
Solid 3*
short dash 1*

03-28-00

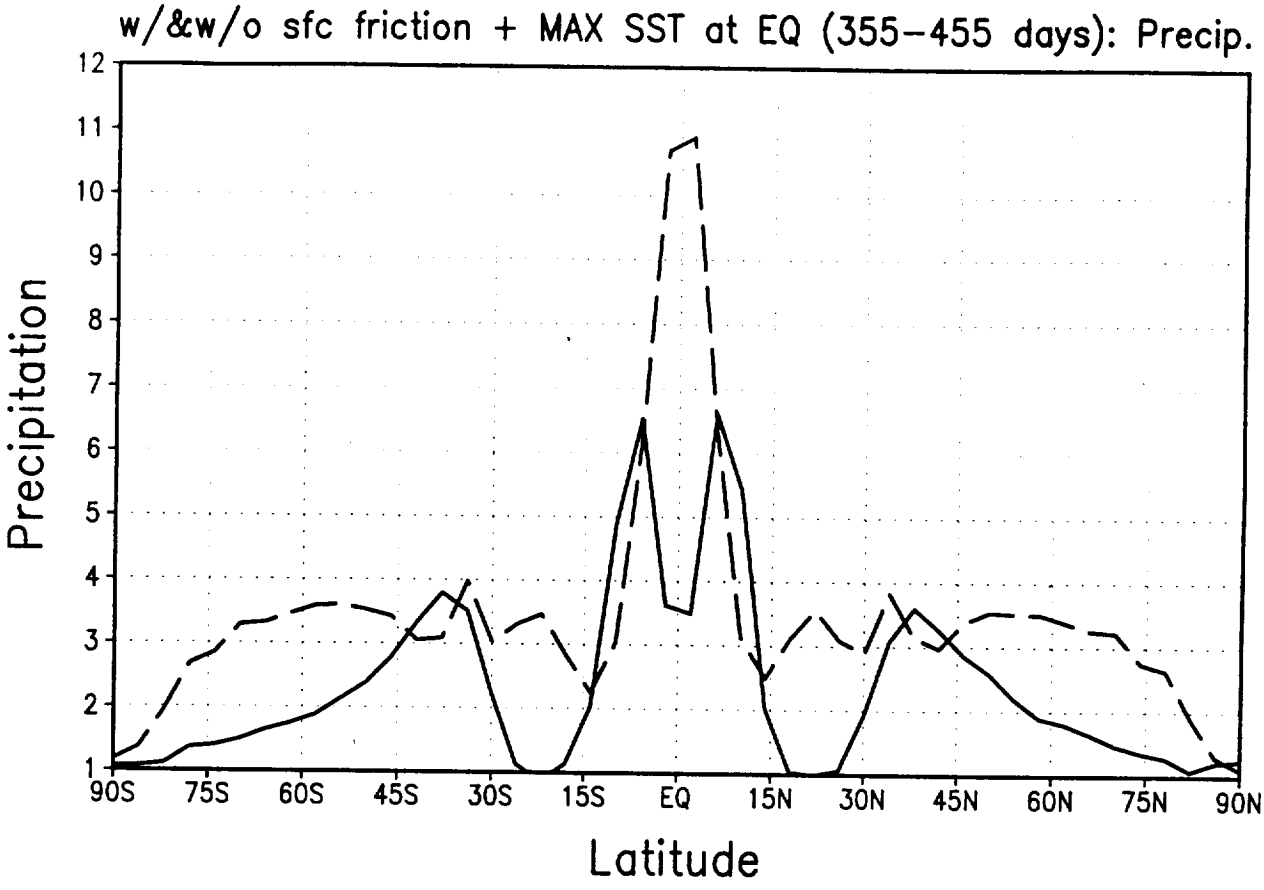

With Gaussian SST

RHS solid w s/c friction
dash w/o

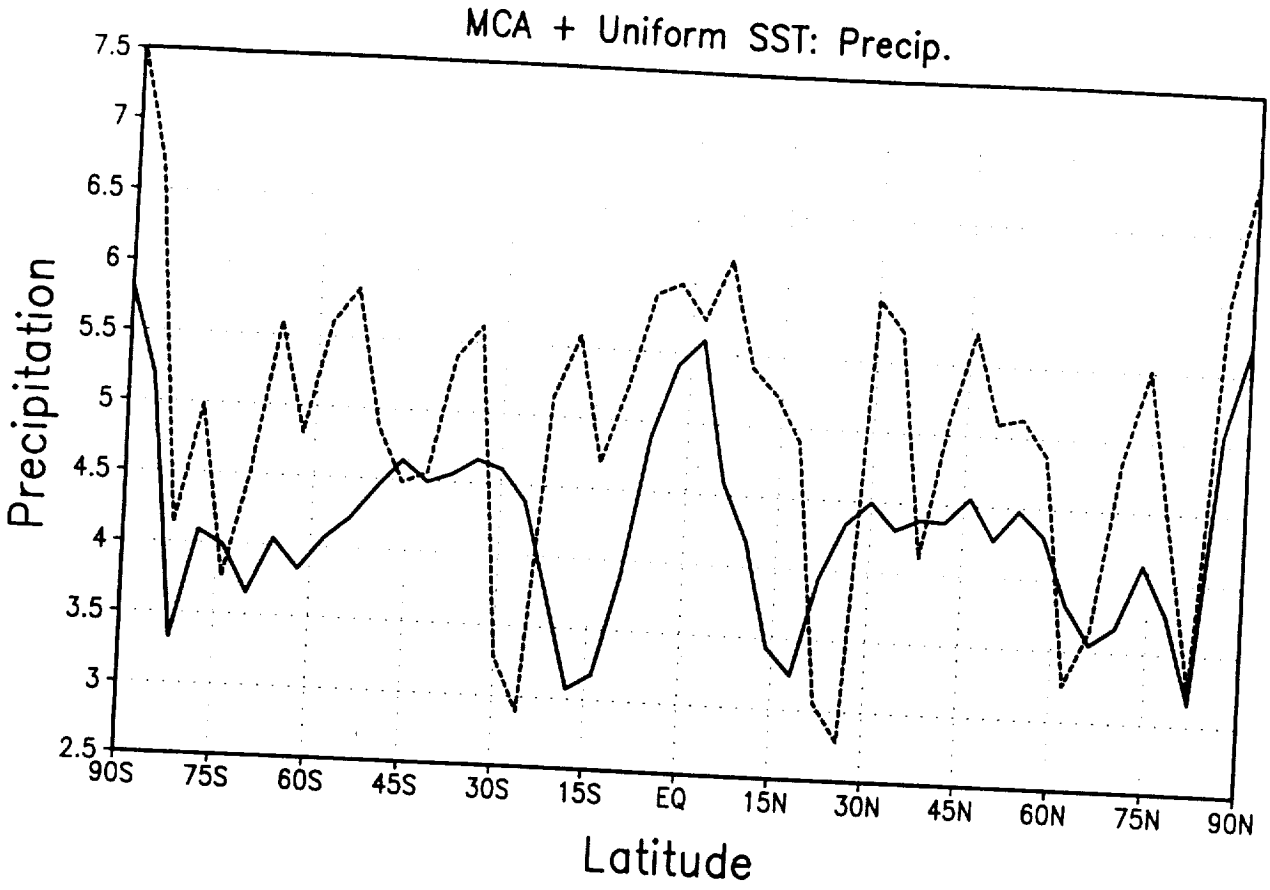
MCA + Uniform SST: Precip.
Precipitation
7.5
7
6.5
6
5.5
5
4.5
4
3.5
3
2.5
90S
75S
60S
45S
30S
15S
EQ
15N
30N
45N
60N
75N
90N
Latitude